

Table of contents

**Supplementary Fig. 1 | Sensitivity studies**

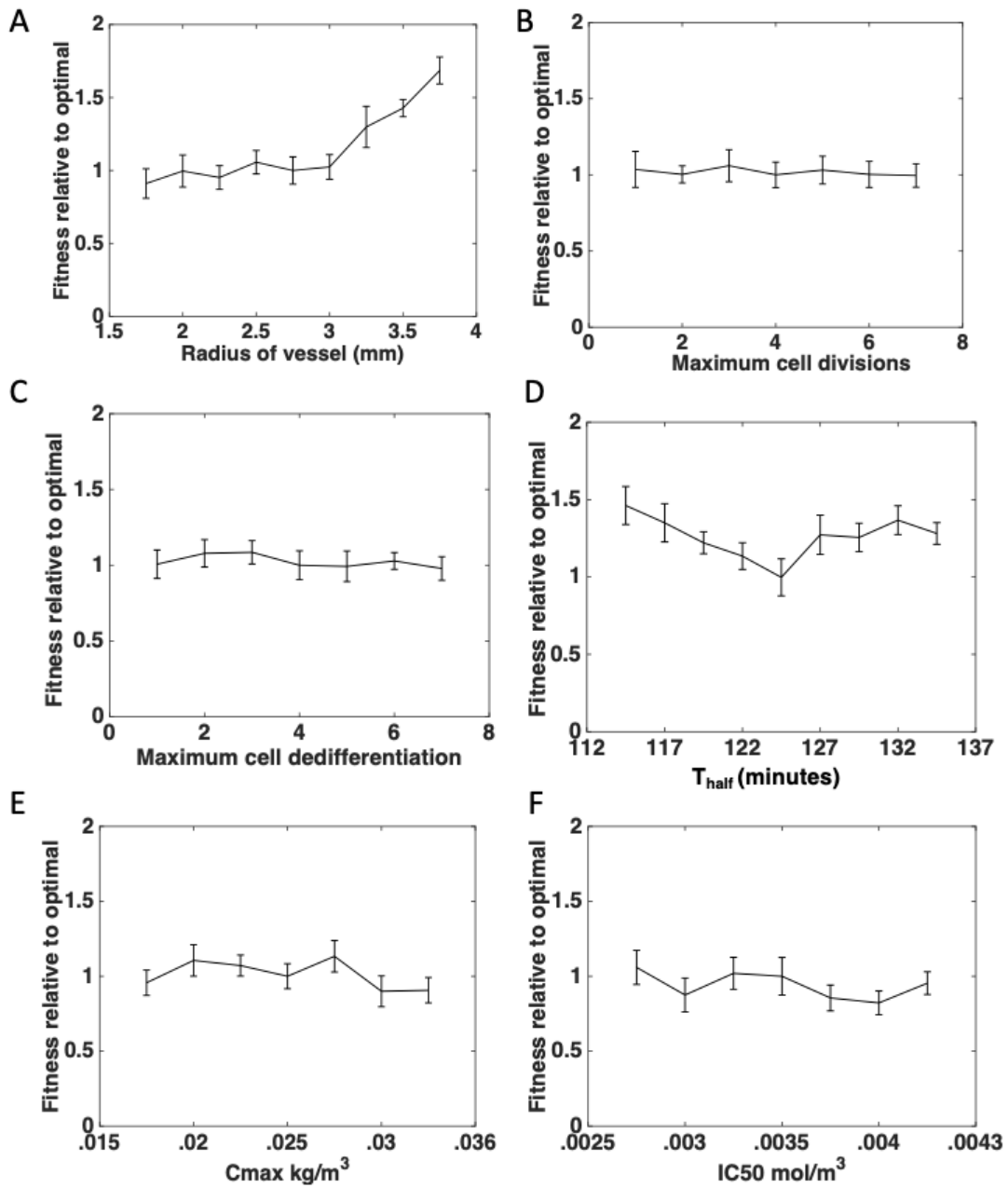
**Supplementary Fig. 2 | Radiosensitivity studies**

**Supplementary Fig. 3 | Prediction of GBM growth and treatment response with chemoradiation resistance**

**Supplementary Fig. 4 | The emergence of chemoradiation resistance**

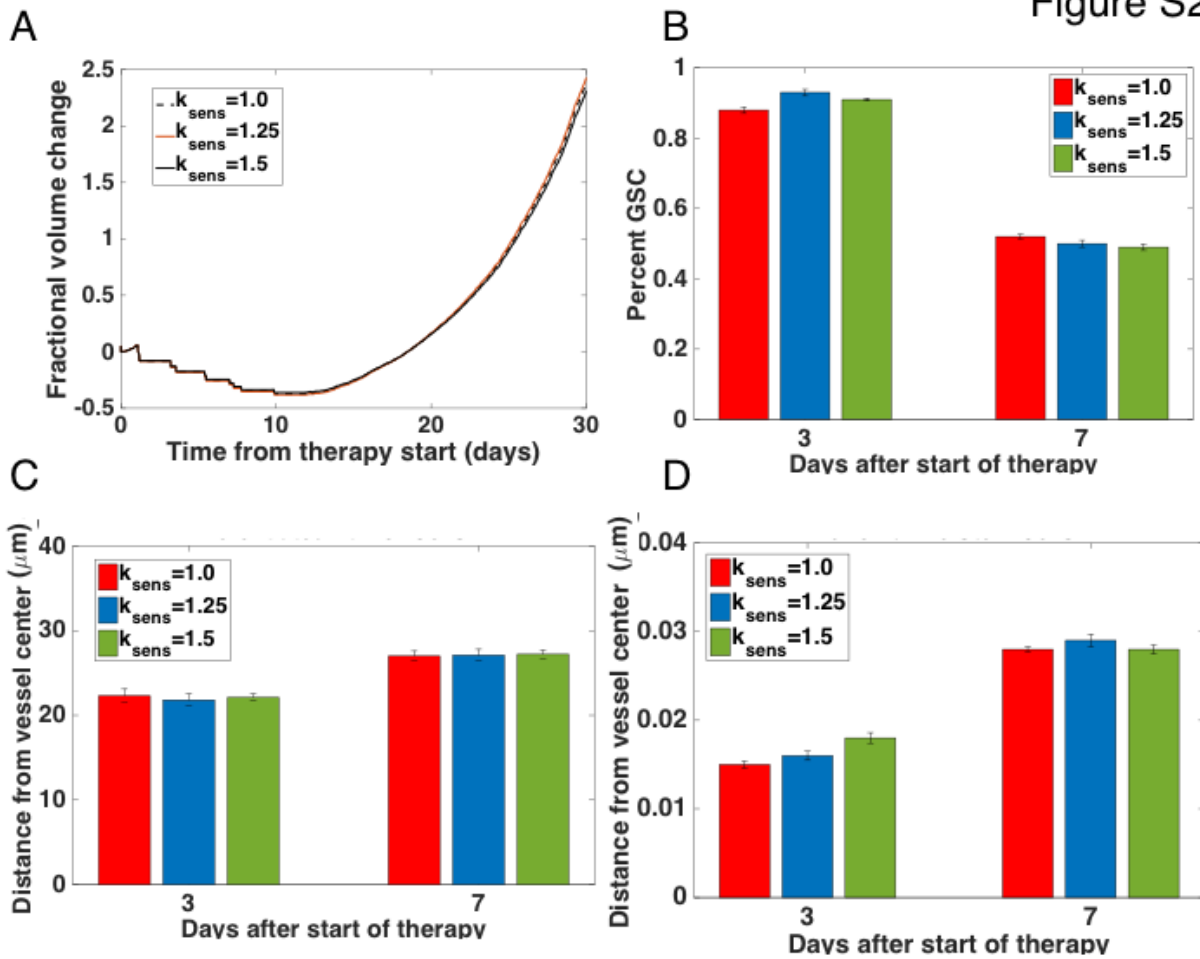
**Supplementary Table 1 | Description and values of the mathematical model parameters**

Figure S1



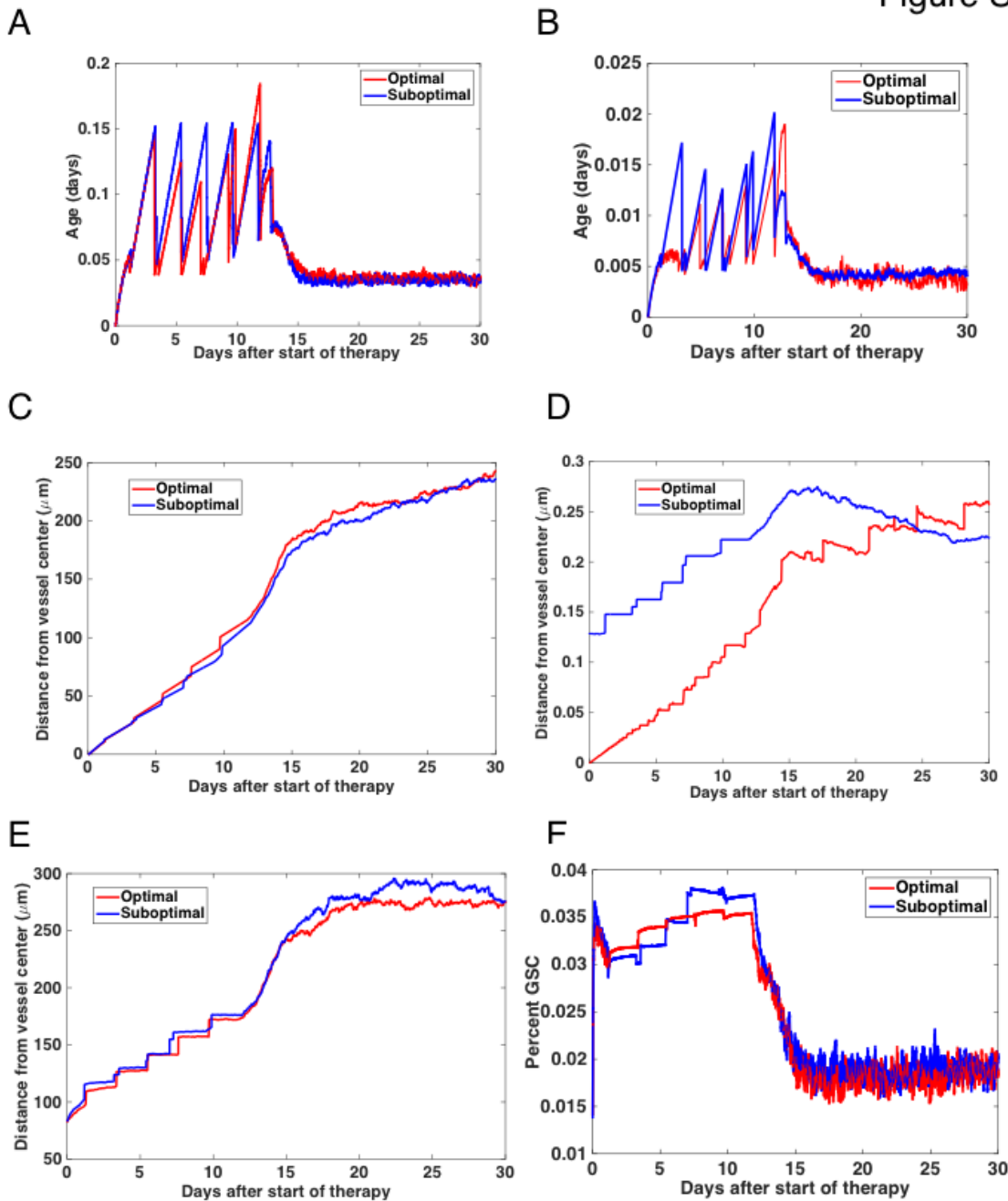
**Supplementary Figure 1 | Sensitivity studies.** The figure shows the relative efficacy of the fitness of the optimal schedule. To measure relative efficacy, we investigated the ratio of the tumor population under the given parameters to the tumor population under the nominal condition. This comparison was made 30 days after initiation of therapy. In panels (A-F) we varied parameters  $R_{vessel}$ ,  $Z$ ,  $Z_{revert}$ ,  $T_{max}$ ,  $T_{half}$ ,  $C_{max}$ , and  $IC_{50}$ . To account for stochasticity in the model, each simulation was completed 128 times. Error bars, mean +/- s.d.

Figure S2



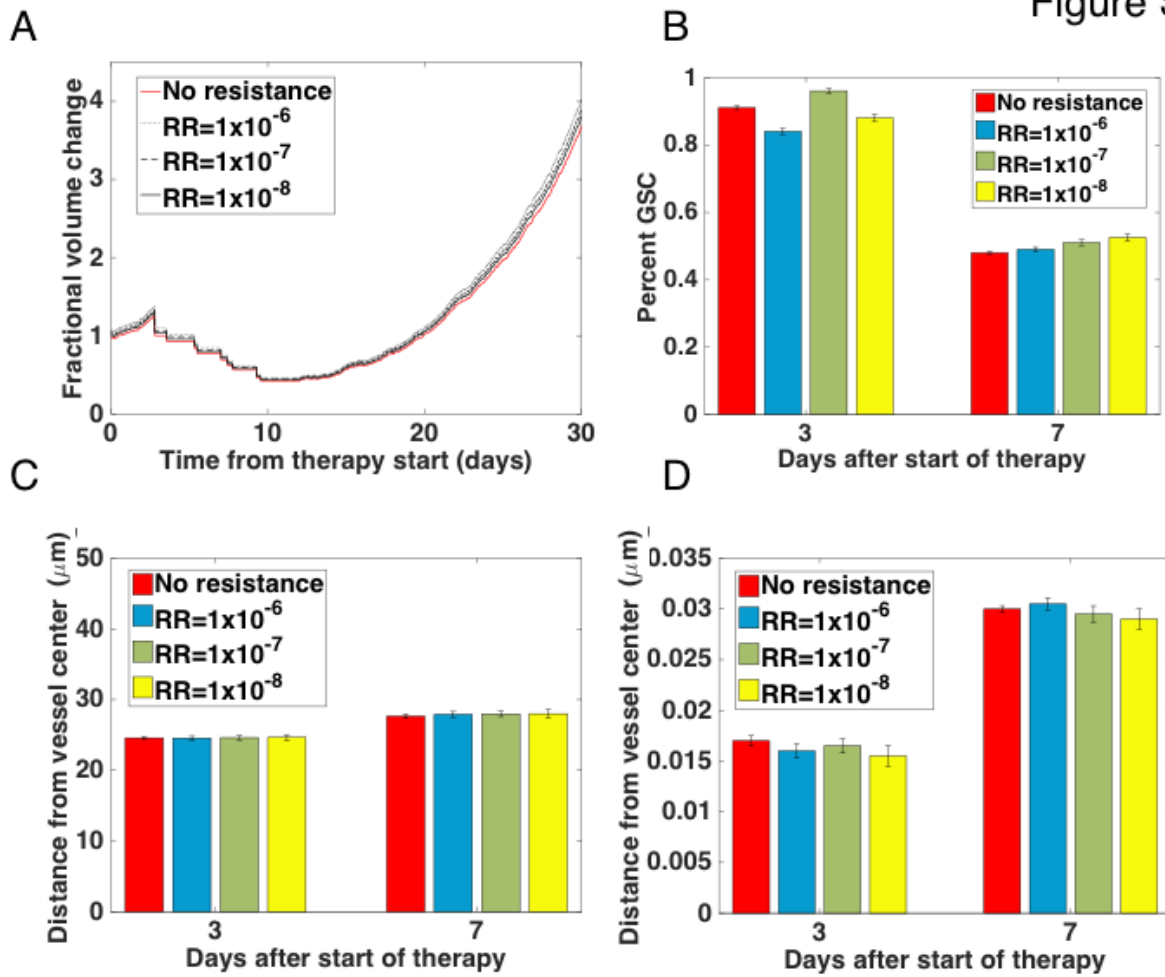
**Supplementary Figure 2 | Radiosensitivity studies.** The figure shows the relative effect on tumor fractional volume change for different time periods between administration of TMZ and radiation. To account for stochasticity in the model, each simulation was completed 128 times. **(A)** Fractional volume change under different settings for the  $k_{sens}$  parameter are depicted. **(B)** Further sensitivity studies are shown looking at the percent of glioma-like stem cells under each  $k_{sens}$  value at two key time points: one day and seven days after start of therapy. Error bars, mean  $\pm$  s.d. **(C-D)** Prediction plots showing the average distance from the vessel center 3 days and 7 days after treatment states for a model with a range of  $k_{sens}$  values. Error bars, mean  $\pm$  s.d. **(C)** shows the results for GSCs and **(D)** DTCs.

Figure S3



**Supplementary Figure 3 | Prediction of GBM growth and treatment response with chemoradiation resistance. (A-B)** Plots showing the average age of the cells at up to 30 days after the treatment started. **(A)** shows the results for GSCs and **(B)** DTCs. **(C-D)** Prediction plots showing the average distance from the vessel center up to 30 days after treatment commences. **(C)** shows the results for GSCs and **(D)** for DTCs. **(E)** Maximum distance from the vessel that any of the cells travel up to 30 days after treatment commences. **(F)** Percent of cells that are GSC up to 30 days after treatment initiation.

Figure S4



**Supplementary Figure 4 | The emergence of chemoradiation resistance.** The figure shows the effects of the emergence of therapy-resistant cells. **(A)** Plot showing the expected fractional volume change over time for the optimized schedule from **Table 1A** without the inclusion of resistant cells versus models with the resistance rate set to a range of values. **(B)** Percent of cells that are GSC at 3 and 7 day after treatment starts. Error bars, mean +/- s.d. **(C-D)** Prediction plots showing the average distance from the vessel center 3 days after treatment starts and 7 days after treatment starts for a model with a range of resistance rate settings. Error bars, mean +/- s.d. **(C)** shows the results for DTCs and **(D)** for GSCs.

**Supplementary Table S1 | Description and values of the mathematical model parameters.** Note that no single source was available to quantify all parameters and their variability; to address this limitation we performed sensitivity analyses of the parameters as outlined in the methods. Note also that the values of  $\alpha_d$  and  $\alpha_s$  might represent a lower bound.

<b>Biological Process</b>	<b>Symbol</b>	<b>Value</b>	<b>Method</b>	<b>Citation</b>
Per Gy production of lethal DNA lesions from single radiation track in DSC and SLRC	$\alpha_d/\alpha_s$	0.0987/0.00987	inferred	<sup>18</sup>
Per Gy <sup>2</sup> production of lethal DNA lesions from two radiation tracks in DSC and SLRC	$\beta_d/\beta_s$	$1.14 \times 10^{-7} / 1.14 \times 10^{-8}$	inferred	<sup>18</sup>
Rate at which newly converted DSC leads to clonal expansion (hr)	$\eta_d$	0.054	inferred	
Minimum time for newly converted DSC to begin clonal expansion (hr)	$M_d$	24	inferred	<sup>18</sup>
Minimum time DSC and SLRC are in quiescence (hr)	$L_d/L_s$	24/36	inferred	<sup>18</sup>
Rate at which DSC and SLRC exit quiescence	$\lambda_d/\lambda_s$	0.1/0.0328	inferred	<sup>18</sup>
Proliferation rate of DSC and SLRC after exiting quiescence	$r_d/r_s$	0.0038/0.008	inferred	<sup>18</sup>
Initial ratio of DSC to SLRC	$R$	20	inferred	<sup>18</sup>
Rate at which SLRC convert to DSC	$\alpha_s$	0.0019	inferred	<sup>18</sup>
Rate of reversion of DSC to SLRC	$\nu$	0.45	inferred	<sup>18</sup>
Fraction of DSC capable of reverting to SLRC	$\gamma$	0.4	inferred	<sup>18</sup>
Time to peak reversion after irradiation	$\mu$	3.25	inferred	<sup>18</sup>
Width of window of reversion	$\sigma^2$	1.46	inferred	<sup>18</sup>
Half-life of chemotherapy	$T_{1/2}$	1.25	PK value	<sup>47</sup>
Maximum concentration of chemotherapeutic in the blood	$C_{max}$	36	PK value	<sup>14</sup>
Timepoint of maximum chemotherapeutic concentration (hrs)	$T_{max}$	0.5	PK value	<sup>14</sup>
Number of times a cell can dedifferentiate	$z_{revert}$	7	Sensitivity analysis	this work
Molecular weight of TMZ	$MW$	194.12	PK value	<sup>42</sup>
EC50 for TMZ (mol/m <sup>3</sup> )	$EC50$	0.004268	PK vlaue	<sup>42</sup>